
Aerodynamic sound generation by turbulence in shear flows

G. Khujadze^{1,3}, G. Chagelishvili^{2,3}, M. Oberlack¹, A. Tevzadze³ and G. Bodo⁴

¹ Chair of Fluid Dynamics, Technische Universität Darmstadt, Germany
khujadze@fdy.tu-darmstadt.de

² M. Nodia institute of Geophysics, Tbilisi, Georgia,

³ E. Kharadze Georgian National Astrophysical Observatory, Tbilisi, Georgia

⁴ Osservatorio Astronomico di Torino, Pino Torinese, Italy

The nonlinear aerodynamic sound generation by turbulence has been long analyzed since the foundation of the theory of aerodynamic sound in pioneering paper by Lighthill [1]. Also, it was Lighthill [2] who noted that velocity shear can increase the acoustic wave emission in the aerodynamic situation due to the existence of linear terms in the inhomogeneous part of the analogy equations (second derivative of the Reynolds stress). In [3] it was disclosed and described a linear aerodynamic sound generation mechanism. Specifically, it was shown that the flow non-normality induced linear phenomenon of the conversion of vortex mode into the acoustic wave mode is the only contributor to the acoustic wave production of the unbounded shear flows in the linear regime. From the physical point of view the *potential vorticity* was identified as the linear source of acoustic waves in shear flows.

We perform comparative analysis of linear and nonlinear aerodynamic sound generation by turbulent perturbations in constant shear flows and study numerically the generation of acoustic waves by stochastic/turbulent perturbations embedded in 2D planar unbounded inviscid constant shear flow with uniform background density and pressure ($U_0(Ay, 0)$; $A, \rho_0, P_0 = const$). The governing hydrodynamic equations of the considered 2D compressible flow are:

$$\frac{\partial \rho}{\partial t} + \frac{\partial (\rho U_x)}{\partial x} + \frac{\partial (\rho U_y)}{\partial y} = 0, \quad (1)$$

$$\frac{\partial U_x}{\partial t} + U_x \frac{\partial U_x}{\partial x} + U_y \frac{\partial U_x}{\partial y} = -\frac{1}{\rho} \frac{\partial P}{\partial x}, \quad \frac{\partial U_y}{\partial t} + U_x \frac{\partial U_y}{\partial x} + U_y \frac{\partial U_y}{\partial y} = -\frac{1}{\rho} \frac{\partial P}{\partial y}, \quad (2)$$

$$\left(\frac{\partial}{\partial t} + U_x \frac{\partial}{\partial x} + U_y \frac{\partial}{\partial y} \right) P = -\frac{\gamma P}{\rho} \left(\frac{\partial}{\partial t} + U_x \frac{\partial}{\partial x} + U_y \frac{\partial}{\partial y} \right) \rho, \quad (3)$$

where γ – adiabatic index, $c_s^2 \equiv \gamma P_0 / \rho_0$ – sound speed. The potential vorticity is defined as: $\mathcal{W} = [\text{curl} \mathbf{U}]_z / \rho$.

Only stochastic streamwise and crossstream perturbation velocities are embedded in the flow at $t = 0$:

$$u_x(x, y, 0) \neq 0; \quad u_y(x, y, 0) \neq 0; \quad \rho'(x, y, 0) = 0; \quad P'(x, y, 0) = 0. \quad (4)$$

The embedded perturbation is localized in the crossstream direction and it is homogeneous in the streamwise direction. $u_x(x, y, 0)$ and $u_y(x, y, 0)$ are defined by the following stream function:

$$\psi(x, y, 0) = B \exp\left(-\frac{y^2}{L_l^2}\right) \int_{-\infty}^{+\infty} dk_x dk_y \left(\frac{k_x k_y}{k_0^2}\right)^4 \exp\left(-\frac{k_x^4 + k_y^4}{k_0^4}\right) \times \exp(ik_x x + ik_y y) \zeta(k_x, k_y), \quad (5)$$

$$u_x(x, y, 0) = \frac{\partial}{\partial y} \psi(x, y, 0), \quad u_y(x, y, 0) = -\frac{\partial}{\partial x} \psi(x, y, 0),$$

where $\zeta(k_x, k_y)$ is random number in the range $[0, 1]$ different for different k_x and k_y ; L_l – the localization scale in the crossstream direction; k_0 – the peak center in the streamwise wavenumber K_x axis. The half-width of the spectrum of the inserted perturbation meets the condition $\Delta k_0 \ll k_0$, that allows to discriminate linearly and nonlinearly generated acoustic waves and, thus, to carry out comparative analysis of linear and nonlinear aerodynamic sound generation by turbulent perturbation. The perturbations are inserted in the flow in the physical plane at the parameters $B = 0.5 \times 10^4$; $L_l = 3$; $k_0 = 10$; $c_s = 1$; $A = 4$ at $t = 0$. Simulations were performed using the hydrodynamics module of the PLUTO code [4]. The domain and the grid were $-10 \leq x, y \leq 10$ and 1024×1024 respectively. Finer grid (2048×2048) was used to test the results of the simulations. Dissipative effects are only those related to the use of a mesh of finite width Euler equations are solved using the PLUTO code.

A fault of acoustic analogy treatment in the identification of the true linear sources of aerodynamic sound

The specificity of the acoustic analogy approach is that results strongly depend on the form of the analogy equation as well as on the aero-acoustic variable chosen to analyze the process. This is more essential when the convective terms are important and the model should take into account the background flow. Hence, the acoustic analogy equation have been the subject to various approximations in order to take into account the effect of the background inhomogeneous flow correctly. However, identification of the true sources of aerodynamic sound remains relevant [5]. Discussing the true linear sources of aerodynamic sound, we compare the linear acoustic wave production in the unbounded shear flows induced by the non-normality of the flow (described in the paper [3]) with the linear part of the acoustic analogy source. The linear part of the acoustic analogy source may be defined as:

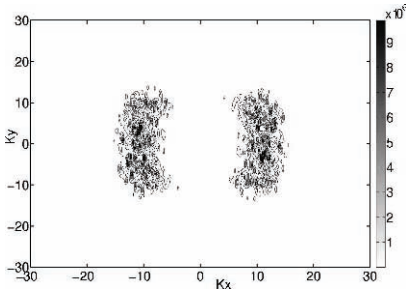


Fig. 1. The linear source of the acoustic analogy equation at $t = 0$ in the wavenumber plane ($S^{(l)}(k_x, k_y, 0)$).

$$S^{(l)} = 2 \frac{\partial^2}{\partial x^2} (\rho_0 A y u_x) + 2 \frac{\partial^2}{\partial x \partial y} (\rho_0 A y u_y) . \tag{6}$$

The spectrum of the source ($S^{(l)}(k_x, k_y)$) in our case at $t = 0$ is presented in Fig. 1. It shows that the acoustic analogy linear source is distributed in all quadrants of the wavenumber plane. I.e. the linear source generates acoustic field with $k_x k_y < 0$ too. However, according to [3] density perturbation is generated at $k_y \leq k_x$ and the linear generation of acoustic wave Spatial Fourier Harmonics (SFH) by the related vortex mode SFH takes place just at the moment of the crossing of the K_x axis by the last one. Consequently, the acoustic analogy linear source located in the quadrants II and IV (and having $k_x k_y < 0$) is the fault of acoustic analogy treatment. In our opinion, this is a very important conclusion of our research.

Comparative analysis of linear and nonlinear aerodynamic sound generation by turbulent perturbations

The energy of the linearly generated acoustic waves is defined by the mean flow shear parameter and the potential vorticity of the turbulent perturbations and the spectrum, by the k_x spectrum of the potential vorticity at $k_y = 0$. The nonlinear source we define by the nonlinear part of the acoustic analogy source:

$$S^{(nl)} = \frac{\partial^2}{\partial x^2} (\rho u_x^2) + 2 \frac{\partial^2}{\partial x \partial y} (\rho u_x u_y) + \frac{\partial^2}{\partial y^2} (\rho u_y^2) . \tag{7}$$

The spectrum of these sources at $t = 0$ are presented in Figs. 2 and 3. Fig. 2 shows that the potential vorticity of the perturbations along K_x axis is located in a streamwise wavenumber range $[k_0 - \Delta k_0, k_0 + \Delta k_0]$. Consequently, the linear aerodynamic sound should be located in the same range of k_x . At the same time Fig. 3 shows that $S^{(nl)}(k_x, k_y, 0)$ is located in a range $[2k_0 - 2\Delta k_0, 2k_0 + 2\Delta k_0]$, i.e. about twice farther than the potential vorticity from the center of the plane.

The density field in the wavenumber plane for parameters $B = 0.5 \times 10^4$; $L_l = 3$; $k_0 = 10$; $c_s = 1$; $A = 4$ at $t = 0.1$ is presented in Fig. 4. The density field in the physical plane for the same parameters at $t = 2$ (in basic unites [m] and [sec]) is presented on Fig. 5. Fig. 4 shows that the

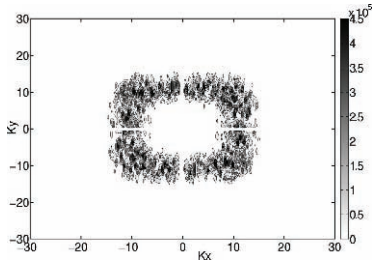


Fig. 2. The potential vorticity field at $t = 0$ in the wavenumber plane.

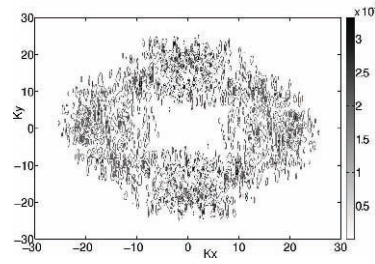


Fig. 3. The acoustic analogy nonlinear source at $t = 0$ in the wavenumber plane ($S^{(nl)}(k_x, k_y, 0)$).

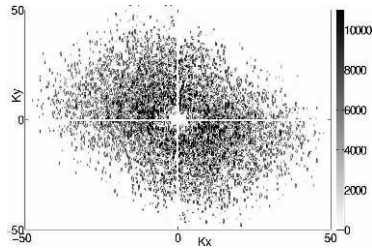


Fig. 4. The density field in the wavenumber plane at $t = 0.1$.

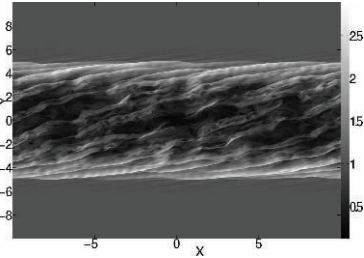


Fig. 5. The density field in the physical plane at $t = 2$.

density field of the perturbations along K_x axis is mainly located around k_0 with an extension to $2k_0$. The density field around k_0 relates to the linear mechanism of the wave generation. The density field close to $2k_0$ relates to the nonlinear mechanism. The figure shows that in the considered case the linear aerodynamic sound is stronger than the nonlinear one. According to Fig. 2, for the considered parameters, the mean flow vorticity is larger than the perturbation potential vorticity – the case when Rapid Distortion Theory (RDT) of turbulence is at work. According to our study the linear aerodynamic sound dominates over nonlinear one at moderate and high shear rates: $R \equiv A/k_0 c_s \geq 0.3$. The dominance of the linear aerodynamic sound occurs up to quite large amplitudes of the turbulent perturbations for which RDT is at work.

References

1. Lighthill M. J.: Proc. R. Soc. London, Ser. A **211**, 564 (1952).
2. Lighthill M. J.: Proc. R. Soc. London, Ser. A **222**, 1 (1954).
3. Chagelishvili G., Tevzadze A., Bodo G. et al.: Phys.Rev.Lett. **79**, 3178 (1997).
4. Mignone A., Bodo G., Massaglia S. et al.: Astroph. JS, **170**, 228, (2007).
5. Goldstein M. E.: J. Fluid Mech. **526**, 337, (2005).